

Strength of thin plate girders with circular or rectangular web holes without web stiffeners

Autor(en): **Höglund, Torsten**

Objektyp: **Article**

Zeitschrift: **IABSE reports of the working commissions = Rapports des commissions de travail AIPC = IVBH Berichte der Arbeitskommissionen**

Band (Jahr): **11 (1971)**

PDF erstellt am: **14.08.2024**

Persistenter Link: <https://doi.org/10.5169/seals-12073>

Nutzungsbedingungen

Die ETH-Bibliothek ist Anbieterin der digitalisierten Zeitschriften. Sie besitzt keine Urheberrechte an den Inhalten der Zeitschriften. Die Rechte liegen in der Regel bei den Herausgebern.

Die auf der Plattform e-periodica veröffentlichten Dokumente stehen für nicht-kommerzielle Zwecke in Lehre und Forschung sowie für die private Nutzung frei zur Verfügung. Einzelne Dateien oder Ausdrucke aus diesem Angebot können zusammen mit diesen Nutzungsbedingungen und den korrekten Herkunftsbezeichnungen weitergegeben werden.

Das Veröffentlichen von Bildern in Print- und Online-Publikationen ist nur mit vorheriger Genehmigung der Rechteinhaber erlaubt. Die systematische Speicherung von Teilen des elektronischen Angebots auf anderen Servern bedarf ebenfalls des schriftlichen Einverständnisses der Rechteinhaber.

Haftungsausschluss

Alle Angaben erfolgen ohne Gewähr für Vollständigkeit oder Richtigkeit. Es wird keine Haftung übernommen für Schäden durch die Verwendung von Informationen aus diesem Online-Angebot oder durch das Fehlen von Informationen. Dies gilt auch für Inhalte Dritter, die über dieses Angebot zugänglich sind.

III

Strength of Thin Plate Girders with Circular or Rectangular Web Holes without Web Stiffeners

Résistance des poutres à âme mince non-raïdiées, comportant des ouvertures rondes ou rectangulaires

Festigkeit dünnwandiger, unversteifter Blechträger mit runden oder rechteckigen Stegaussparungen

TORSTEN HÖGLUND

Techn. lic.

Department of Building Statics and
Structural Engineering of The Royal
Institute of Technology
Stockholm, Sweden

1. INTRODUCTION

The thin plate I-girder has become a frequently used element in roof constructions. This has been possible by the use of rational methods of fabrication and design. One essential point is to avoid web stiffeners, which have to be manually fitted and welded and thus cause considerable costs.

In modern buildings there are often a lot of service ducts and pipings which due to limited construction height intersect the steel structure. The necessary holes in the girder webs have previously been reinforced, mainly due to the lack of knowledge of the buckling conditions of perforated webs. In order to cut costs web stiffeners should be avoided even at such weakenings as holes in the web.

The web of rolled beams are thick and it is usually sufficient to check the stress concentrations around the holes. For thin plate girders web buckling at the holes has to be considered. Only if the postbuckling strength is made full use of web stiffeners around large holes can be avoided in plate girders with thin web.

Very few investigations about buckling of thin plate girder webs with holes has been published [1] and the author has not found any theoretical investigations of the postbuckling strength in the literature. This paper deals with experimental and theoretical study of the strength of statically loaded plate I-girders with circular or rectangular web holes. Girders with very thin web are treated. A more extensive report has been published in Swedish [3]. The distance between holes and web stiffeners is supported to be so large that the web alone must prevent the flanges from vertical buckling.

2. TEST PROGRAM AND TEST PROCEDURE.

A series of four girders of structural carbon steel with two, three or four holes in the web of each girder were tested, see fig. 1. The depth to thickness ratios of the web ranged from 200 to 300, cf fig. 2. The holes were placed in sections loaded in shear only, bending only or a combination of shear and bending.

Table 1. Cross sectional dimensions and constants and yield point of the flange and the web material.

Test girder	h cm	d cm	b cm	t cm	$\frac{h}{d}$	A_w cm ²	I_x cm ⁴	σ_y kp/cm ²	
								flange	web
B2	59,0	0,292	20,2	0,86	202	17,24	36080	2750	3491
B3	59,0	0,293	20,0	0,88	202	17,30	36450	2750	3490
B4	60,0	0,200	15,1	0,61	300	12,00	20520	3040	2800
K1	60,0	0,286	22,6	0,99	210	17,16	46600	2944	4185

The girders were simply supported and loaded with gravity loads in nine or six points with a spacing of 5/3 of the girder depth. The gravity loads were produced by levers and scales with weights, see fig 3.

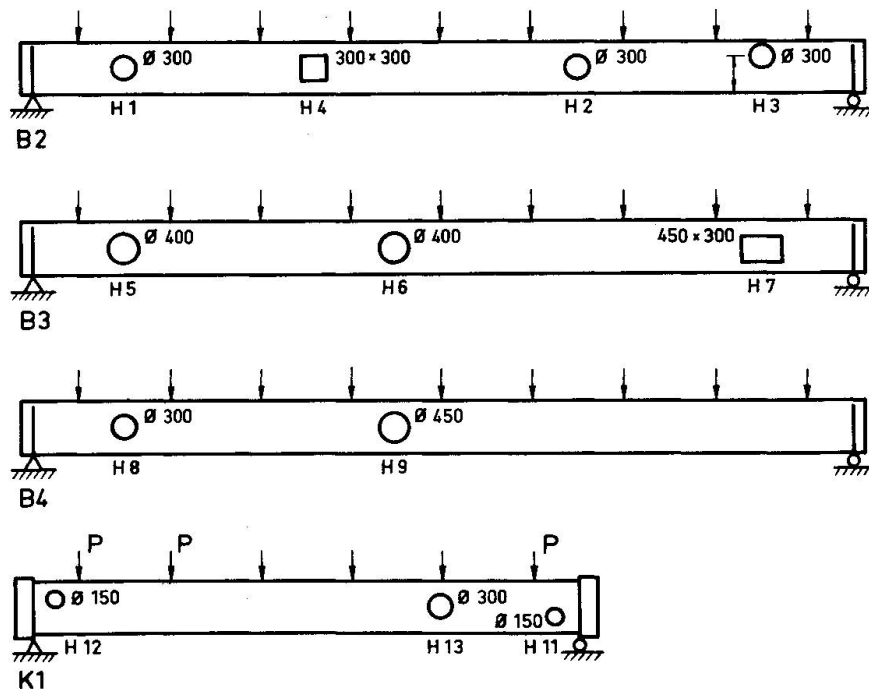


Fig. 1 Test girders

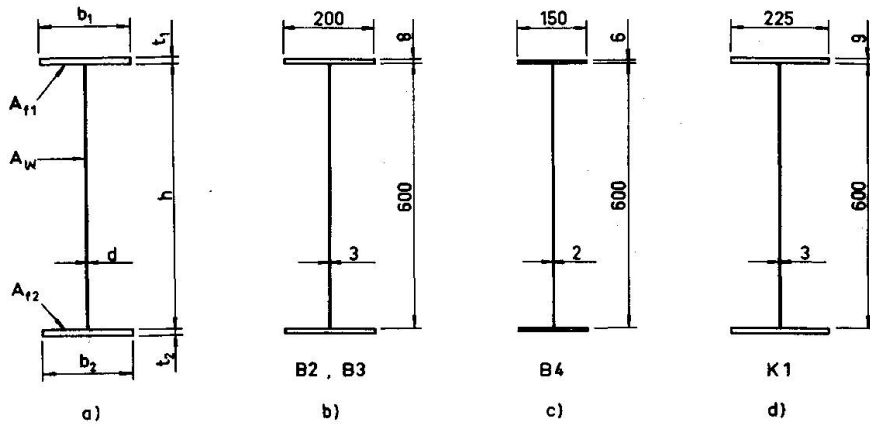
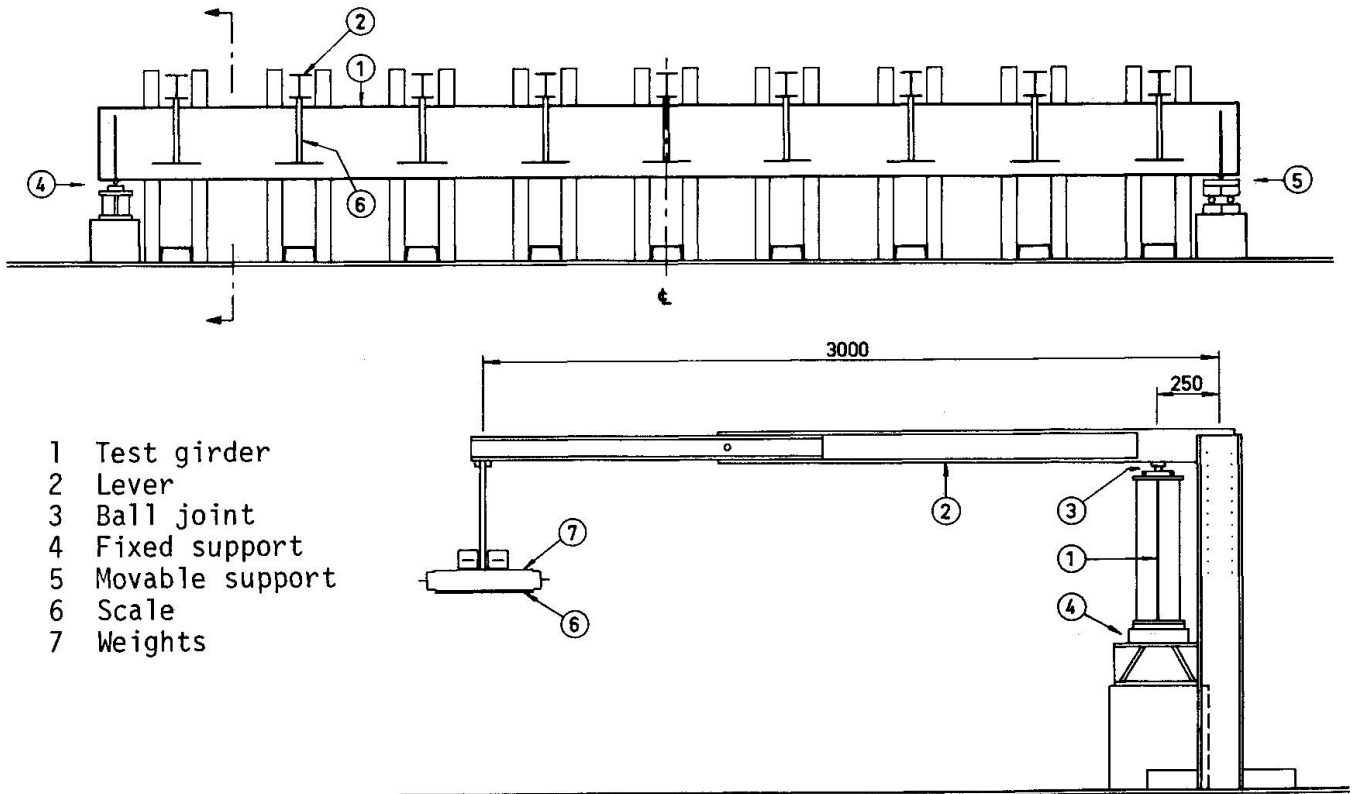


Fig. 2 a) Notations for cross section
 b), c) och d) Girders cross sections for the test girders.

The test girders were fabricated from flamecut flange- and webplates in an automatic welding machine. The holes were sawed and the edges around the holes where grinded. Details of the test girders are given in table 1.

The surface strains at points around the holes in the web and in the flanges were measured with electrical strain gauges. The web deflections near the holes and the centerline deflection were measured with dial gauges.



- 1 Test girder
- 2 Lever
- 3 Ball joint
- 4 Fixed support
- 5 Movable support
- 6 Scale
- 7 Weights

Fig. 3 Test setup.

3. TEST RESULT AND THEORY

Fig. 4, 5, 6 and 7 show the load deflection relationships of the test girders. The shear buckling load, P_{TCR} , for the web without holes calculated under the assumption that the web is simply supported, very long and subjected to constant shear, the buckling load in bending $P_{\sigma CR}$ for the mid span of the girders, the load $P_{\sigma SU}$ which gives the bending moment $\sigma_y \cdot 2I/h$ at the center of the girders and the load $P_{\sigma red}$ which gives the reduced bending moment M_{red} according to Basler and Thürlimann [2] are given in the figures.

$$M_{red} = \frac{2I}{h} \sigma_y (1 - 0,0005 \frac{A_w}{A_f} (\frac{h}{d} - 5,7 \sqrt{\frac{E}{\sigma_y}}))$$

In fig. 4, 5, 6 and 7 are also given the ultimate loads for the girder sections with the holes (P_{br}^{HI} for hole H1 and so on). Finally the web deflection configurations at ultimate load and the stiffener arrangements round the holes after a testcycle to ultimate load are indicated in the figures.

Table 2 gives a summary of test results.

In the following some typical results of measured strain distributions and web deflection curves are given.

Table 2 Summary of test results. (1Mp = 2205 lb)

Test girder	Hole	P Mp	T Mp	τ kp/cm ²	M Mpm	σ kp/cm ²	$\frac{\tau}{\tau_y}$	$\frac{\sigma}{\sigma_y}$
B2	H1	2,21	7,73	449	8,84	734	0,223	0,267
	H3	2,27	7,94	461	9,08	753	0,229	0,274
	H4	3,04	4,56	264	27,36	2270	0,131	0,825
	H2	3,25	4,87	283	29,25	2430	0,141	0,883
B3	H7	1,52	5,32	307	6,08	507	0,152	0,184
	H5	1,68	5,88	340	6,72	560	0,169	0,203
	H6	3,02	1,51	87	30,20	2517	0,043	0,915
B4	H8	1,07	3,74	312	4,28	636	0,193	0,209
	H9	1,40	0,70	58	14,00	2080	0,036	0,685
	H9A	2,00	0	0	16,00	2380	0	0,783
K1	H11	4,53	13,60	792	3,40	223	0,328	0,076
	H12	4,77	14,30	834	3,58	234	0,345	0,079
	H13	4,71	9,42	543	16,49	1080	0,229	0,366

3.1 Circular holes.

3.1.1 Shear force.

Fig. 8a shows the distribution of the tangential middle surface strains in the web around the hole H1 which was situated in a girder section essentially subjected to shear. Two stages are shown; one at a load lower than the buckling load and one near the ultimate load. When the load is small the

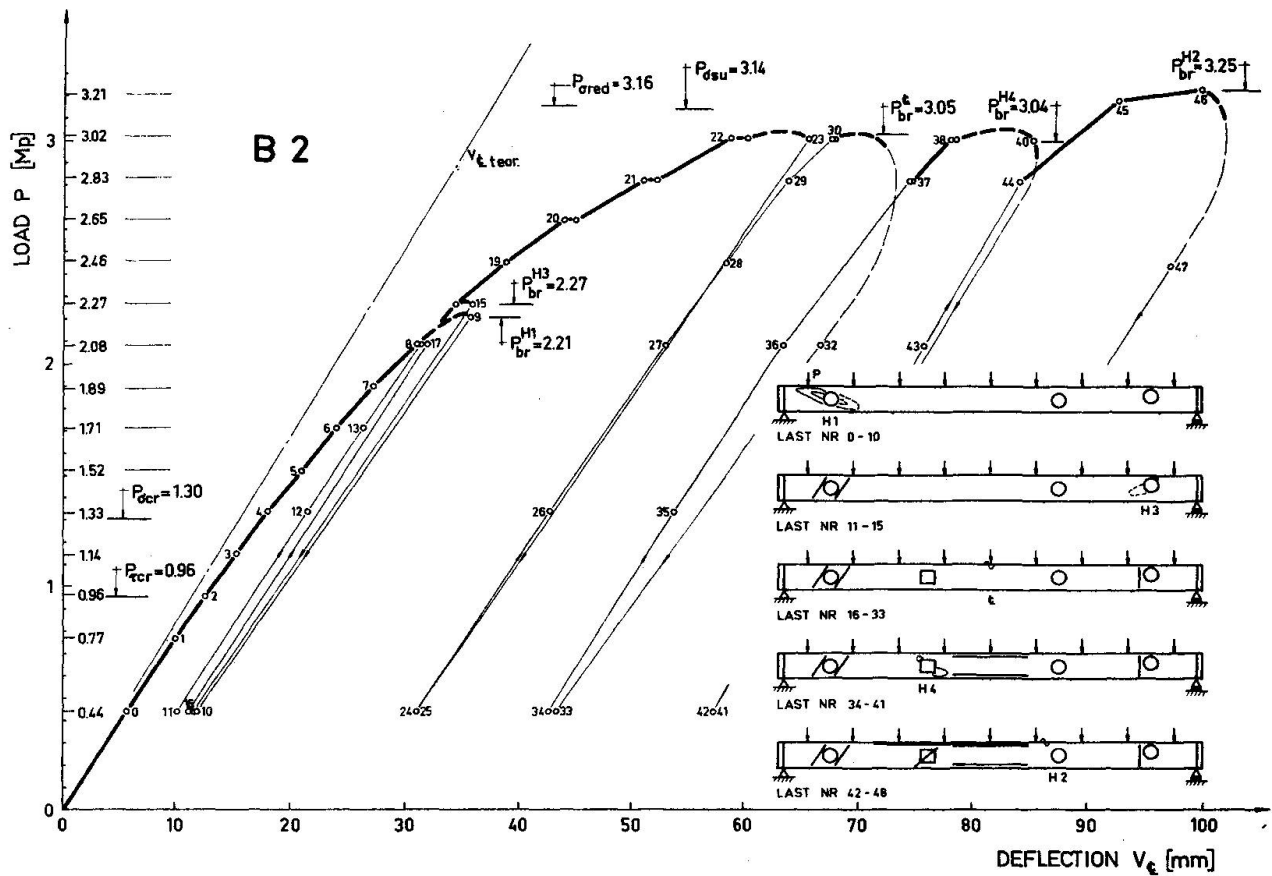


Fig. 4 Load-deflection curve of girder B2.

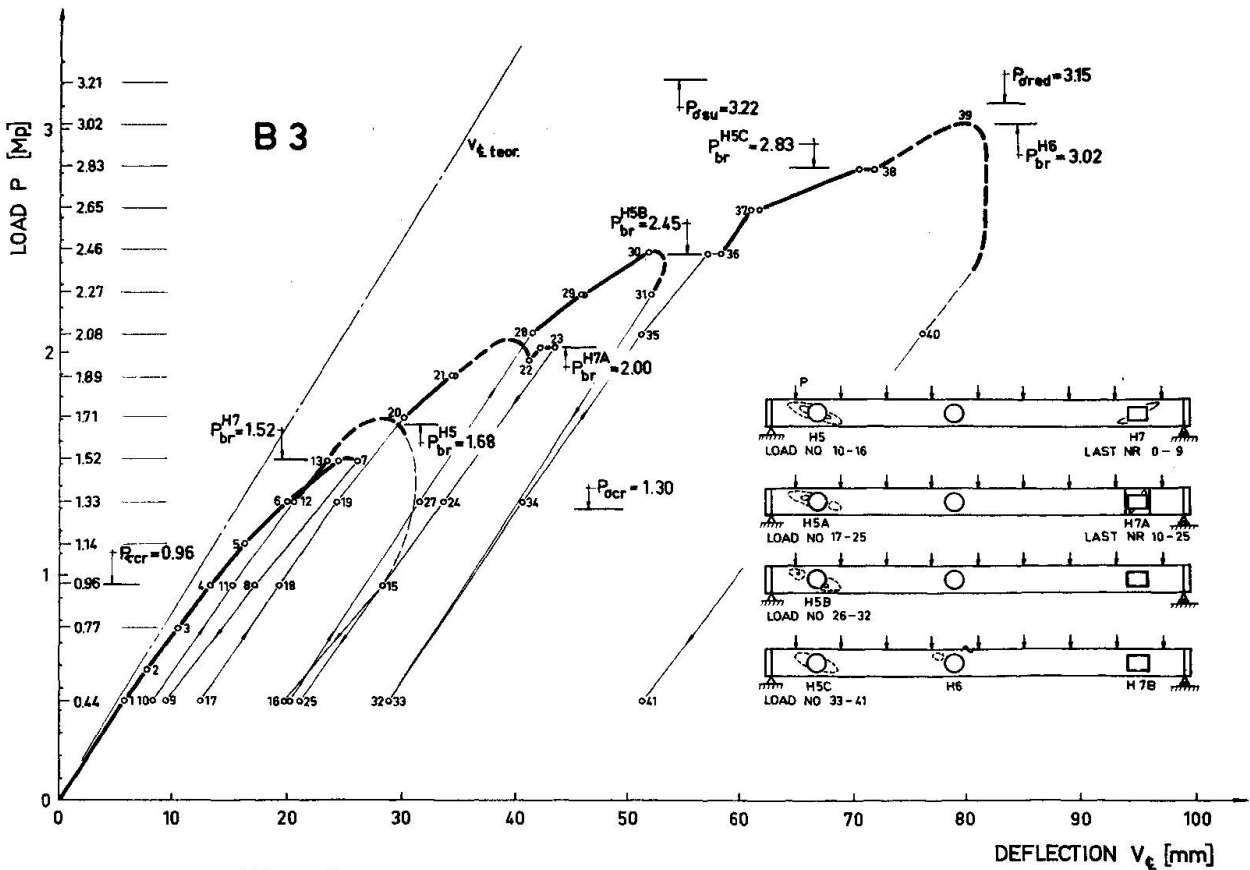


Fig. 5 Load-deflection curve of girder B3.

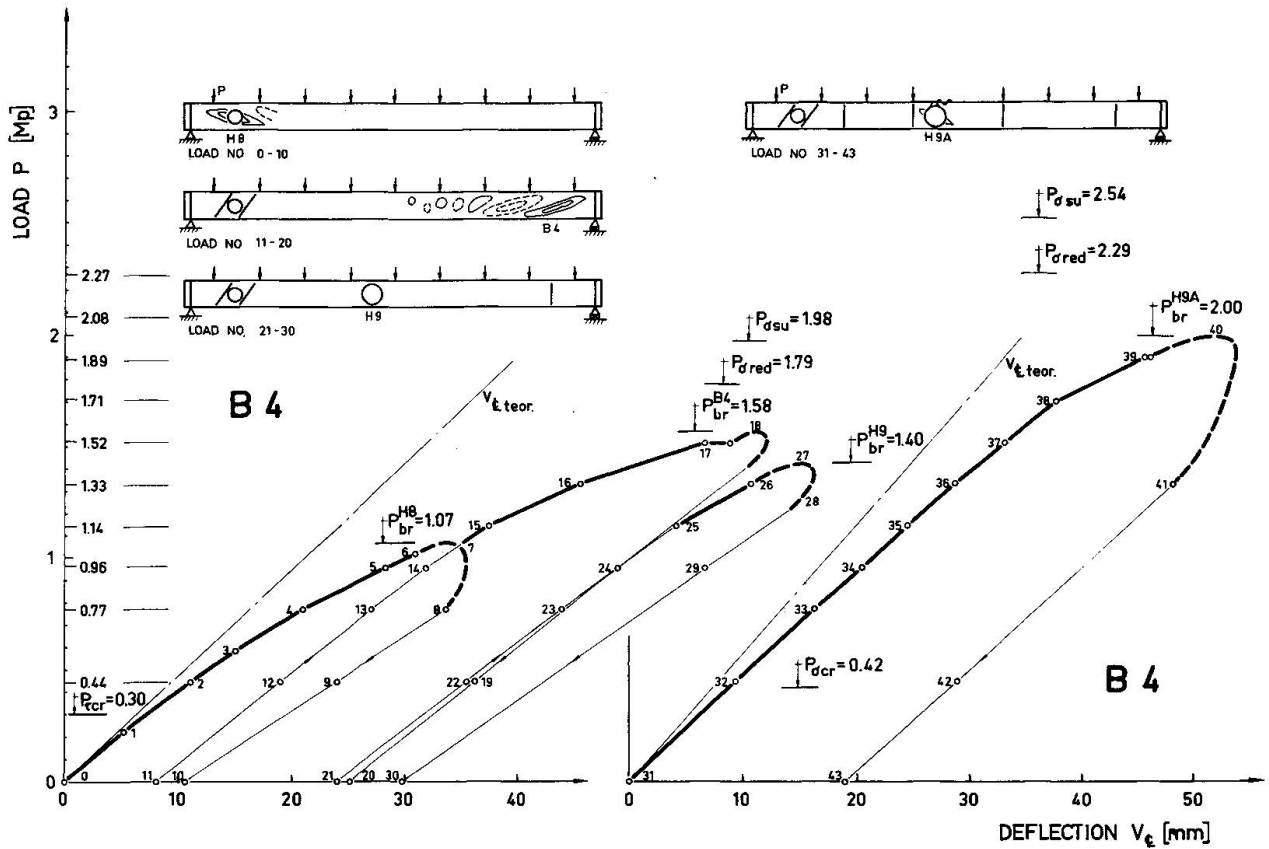


Fig. 6 Load-deflection curve of girder B4.

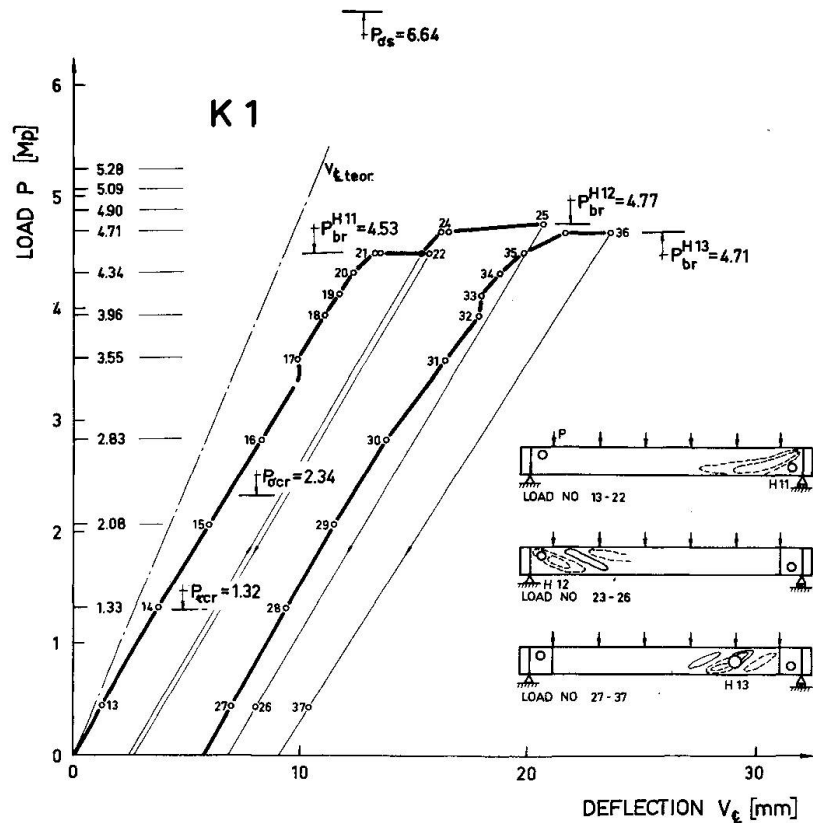


Fig. 7 Load-deflection curve of girder K1.

maximum tangential compressive and tensile strain is about of the same size. When the load is increased the compressive strain remains at a certain level while the tensile strain increases rapidly because of redistribution of stresses after web buckling and lokal yielding.

A model of a shear loaded girder section with a circular hole is shown in fig. 9. The web is supposed to consist of tension fields with the stress equal to the yield stress σ_y and compression fields with a stress estimated as the elastic buckling stress for a web strip with the buckling length ℓ , see fig 9. The inclinations of the tension and compression fields are postulated to be those which furnish the greatest total vertical shear component of the fields.

The diagram in fig. 10 shows curves for the calculated ultimate load as a function of the web slenderness ratio and the size of the hole. The results of the tests of girders with circular web holes in sections essentially loaded in shear are compared with calculated ultimate loads in fig. 10 and in table 3.

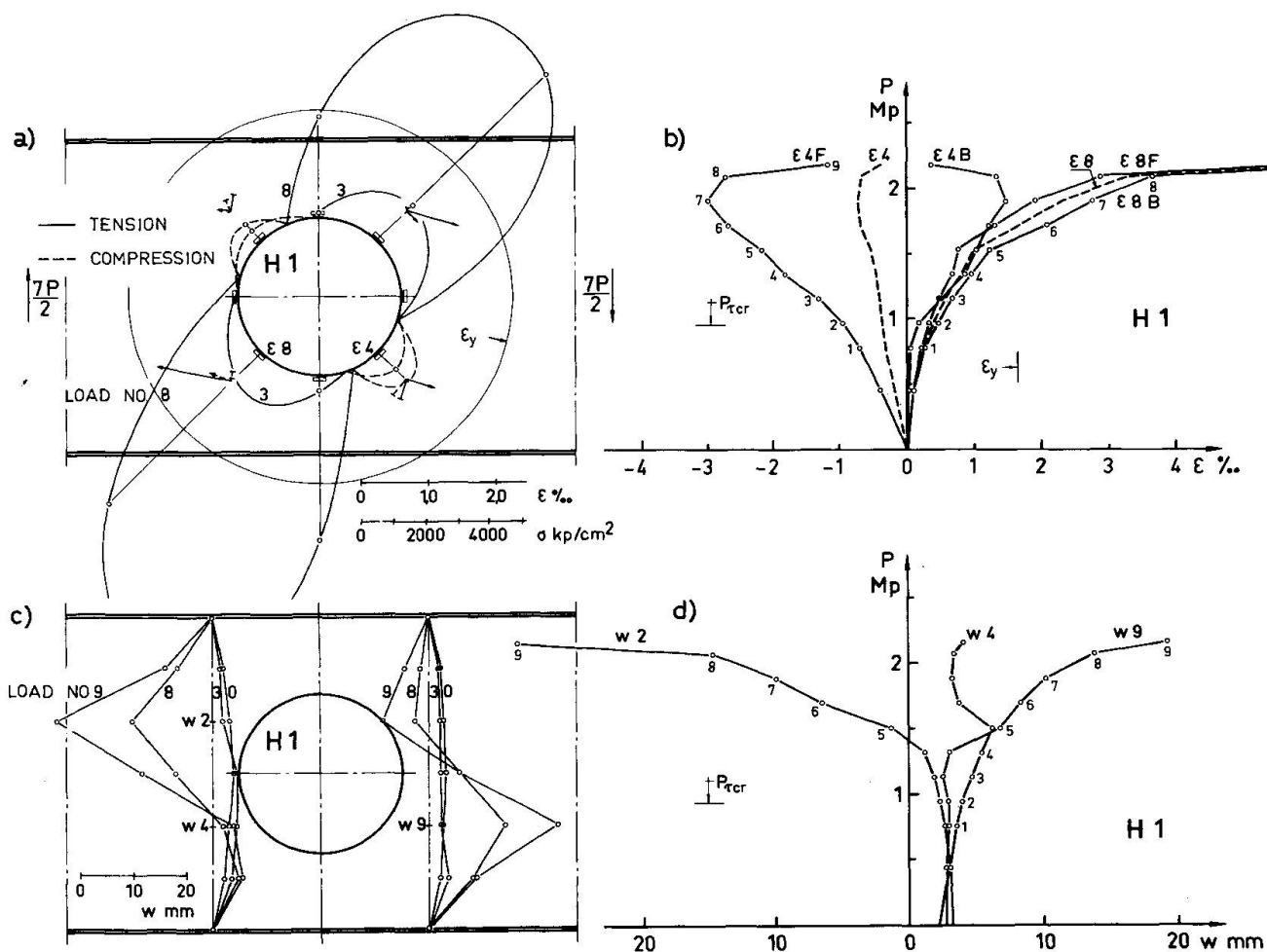


Fig 8 Web strains and web deflections at hole H1.
 a) Tangential mean strains and principal mean stresses in the web evaluated from measurements with strain rosettes.
 b) Tangential strain in the points ϵ_4 and ϵ_8 see fig. a). ϵ_{4f} and ϵ_{8f} are the strains in the front surface, ϵ_{4B} and ϵ_{8B} are the strains in the back surface of the web. The dashed lines marked ϵ_4 and ϵ_8 are the mean stresses in point ϵ_4 and ϵ_8 .
 c) Web deflections in ten points near the hole.
 d) Load-web deflection curves for points w_2 , w_4 and w_9 , see fig. c)

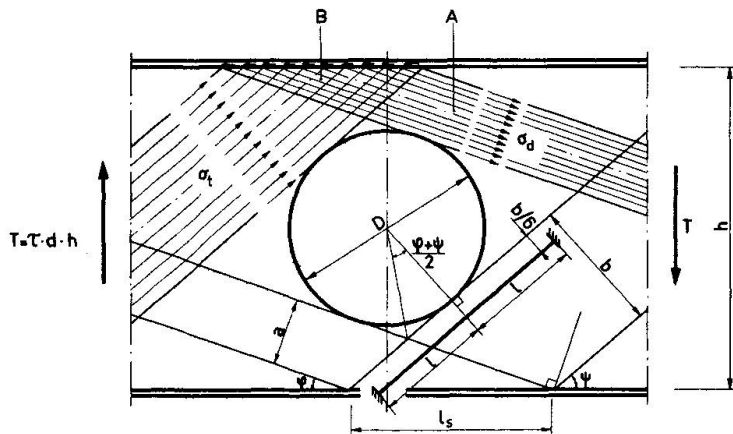


Fig. 9 Model for a girder with a circular web hole subjected to shearing force.

The theory and the tests show that the ultimate shear force is approximately $(1 - D/h)$ times the ultimate buckling shear force for the girder without hole, where D is the diameter of the hole and h is the girder depth.

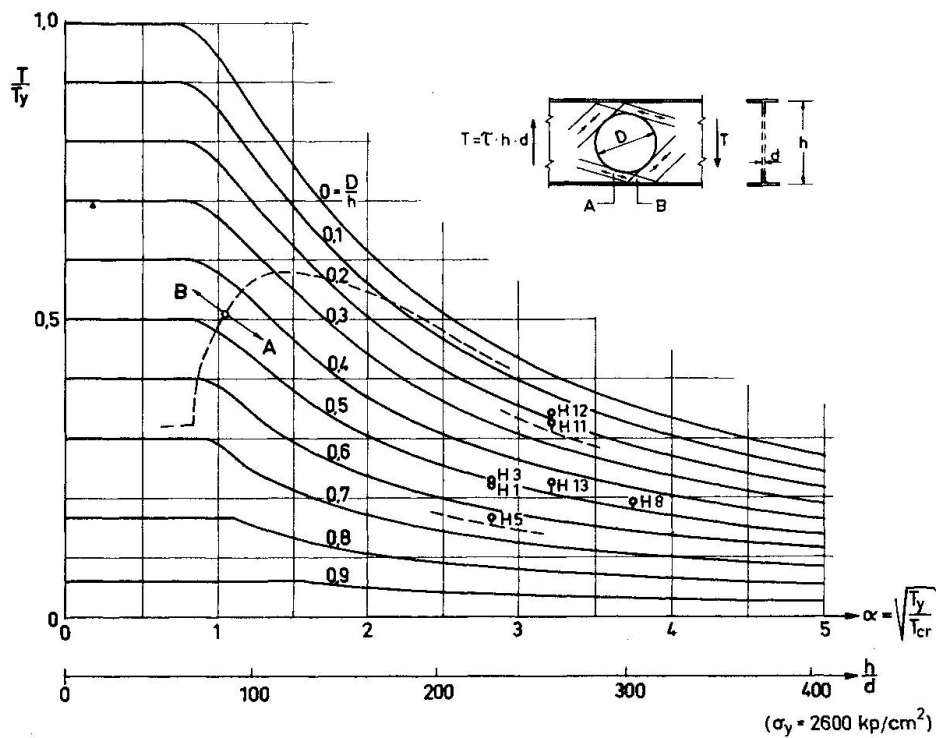


Fig. 10 Calculated ultimate load as a function of hole-size and web slenderness ratio. Circular hole, shear.

Table 3 Summary of test loads and theoretical ultimate loads for girders with circular web holes loaded with shear forces.

Hole	Girder	$\frac{D}{h}$	$\frac{h}{d}$	τ_y a) kp/cm ²	τ_{cr} b) kp/cm ²	α c)	$\frac{T_{th}}{T_y}$ d)	$\frac{T_u}{T_y}$ e)	$\frac{T_u}{T_{th}}$
H1	B2	0,51	202	2015	249	2,85	0,237	0,223	0,94
H3	B2	0,51	202	2015	249	2,85	0,237	0,228	0,96
H5	B3	0,67	202	2015	249	2,85	0,154	0,169	1,10
H8	B4	0,50	300	1617	113	3,78	0,187	0,193	1,03
H11	K1	0,25	210	2416	230	3,24	0,322	0,328	1,02
H12	K1	0,25	210	2416	230	3,24	0,322	0,345	1,07

$$a) \tau_y = \sigma_y / \sqrt{3} \text{ for the web plate}$$

$$d) T_{th} = \text{predicated ultimate load.}$$

$$b) \tau_{cr} = 5,34 \frac{\pi^2 E}{12(1 - \nu^2)} \left(\frac{h}{d}\right)^2$$

$$e) T_u = \text{ultimate test load.}$$

$$c) \alpha = \sqrt{\frac{\tau_y}{\tau_{cr}}}$$

3.12 Bending moment

The distribution of the tangential middle surface strains in the web round the hole H6, situated in a section essentially subjected to bending moment is shown in fig 11a.

A possible mode of action is given in fig. 12. At a distance from the hole the stresses are not influenced of the hole and the stress distribution will be as shown to the right. As the web is thin the stress distribution on the compression side is not triangular. The tension force D_1 and the compression force T_1 corresponding to the parts of the stresses which cannot be transferred through the hole will be transferres downward and upward respectively to the remaining parts of the girder below and above the hole. The conditions of equilibrium leads to compressive stresses along the line B-A' and tensile stresses along A-B', which explains the tangential stress distributions in fig. 11a.

If the web is thin the compressive stress at C may produce buckling of the web, which reduces the compressive stress along B-A' and increases the stress at E.

On the compression side the stresses at E' leads to buckling of the web and an increase of the stresses in the compression flange. Furthermore the web buckling at E' causes an upward deflection of the compression flange above the hole. Downward buckling of the compression flange can take place at a distance from the hole at point A' in fig. 12 but hardly just above the hole.

The reduction of the bending strength of a girder with a centrally placed web hole is usually small because the flanges carry most of the bending moment. For this to be true the size of the hole must be restricted to avoid

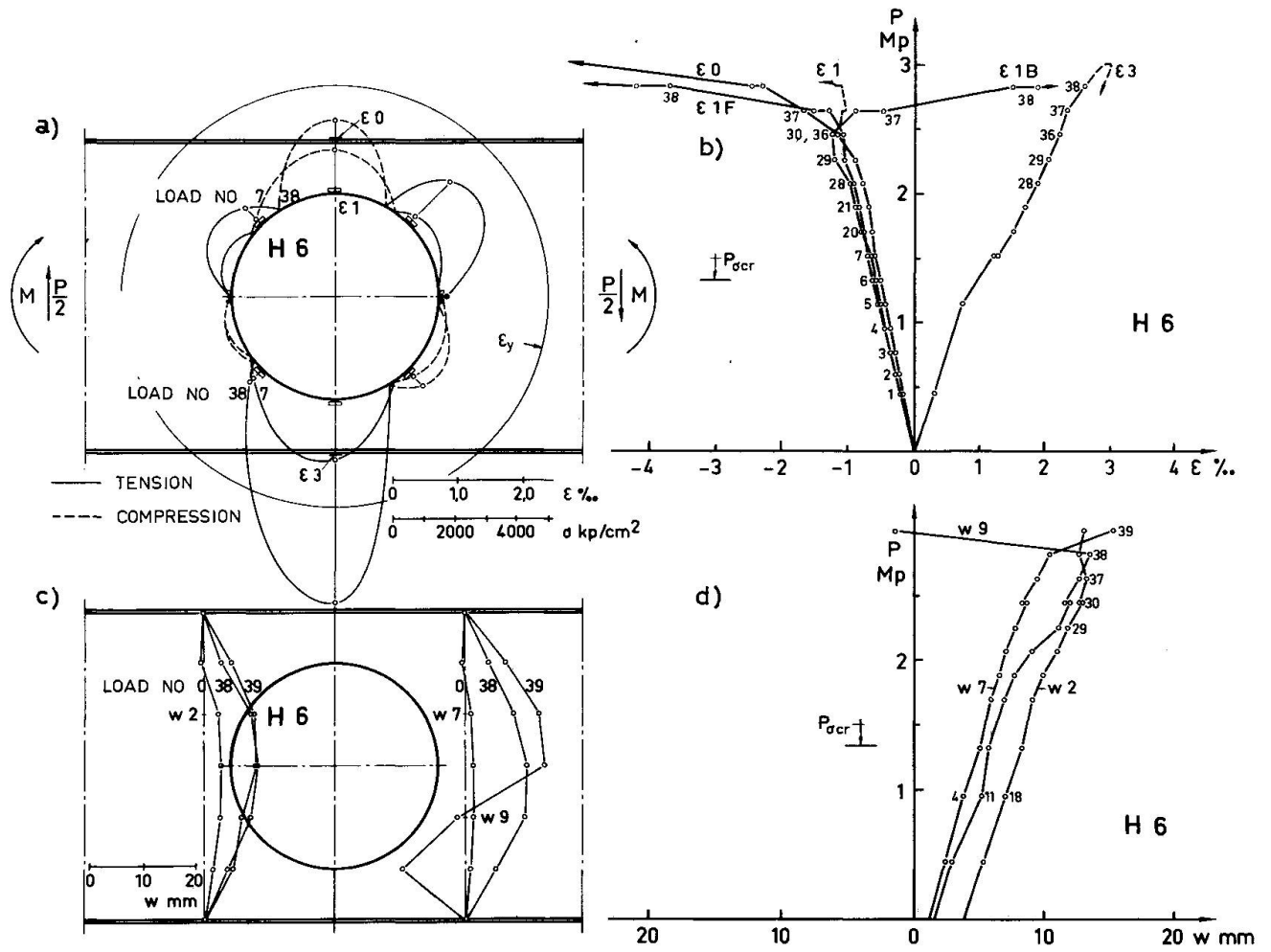


Fig. 11 Web strains and web deflections near hole H6, Notations compare fig 8.

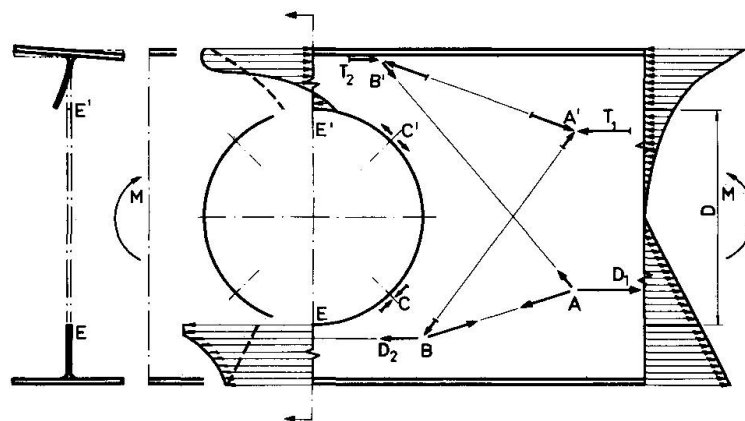
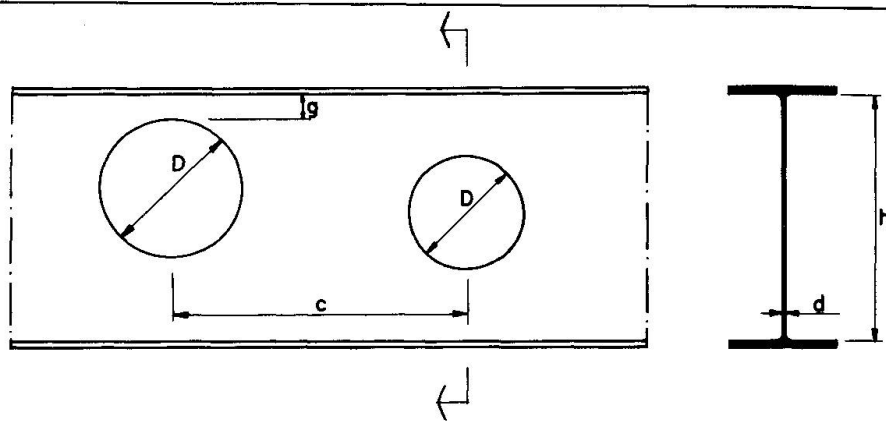


Fig. 12 Stress model for a girder with a circular web hole. Bending moment. torsional buckling, upward or downward vertical buckling and lateral buckling of the compression flange over the hole. Such restrictions are given in fig. 13.



Allowable moment in the section through a hole:

$$M_D = M_{all} \left(1 - \frac{d(h - 2g)^3}{12 \cdot I_x} \right)$$

M_{all} = allowable moment without hole

I_x = moment of inertia for the cross-section without hole.

Allowable shear force in the section through a hole:

$$T_D = \left(1 - \frac{D}{h} \right) T_{all} \quad \text{when } M \leq 0,6 M_D$$

$$T_D = \left(1 - \frac{D}{h} \right) \left(1 - \frac{M}{M_D} \right) \cdot 2,5 \cdot T_{all} \quad \text{when } M > 0,6 M_D$$

where

$$T_{all} = \left(\frac{0,26}{\alpha^2} + 0,10 \right) h \cdot d \cdot \sigma_y \quad \text{when } 1 < \alpha < 2,72$$

$$T_{all} = \frac{1}{\alpha^2} h \cdot d \cdot \sigma_y \quad \text{when } 2,72 < \alpha$$

$$\alpha = 0,35 \frac{h}{d} \sqrt{\frac{\sigma_y}{E}}$$

$$g > 12d$$

$$D < 0,75h$$

$$c > D_{max}$$

Fig. 13 Design rules for thin walled plate girders with circular web holes. [4]

3.13 Shear force and bending moment.

The strength of a plate girder with a hole in a girder section subjected to shearing force and bending moment can be given with an interaction method. Fig. 14 shows possible interaction curves compared with test results.

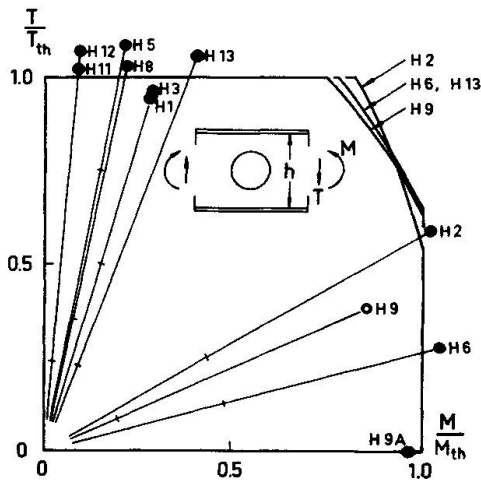


Fig. 14 Comparison between theory and test results for girders with circular holes.

3.2 Rectangular holes.

Stresses and web deflections are concentrated to the corners. A girder with a rectangular web hole may be described as a vierendeel truss with reduced bending capacity of the horizontal and vertical members at the compression corners, see fig. 15.

The risk of vertical buckling or lateral buckling of the compression flange is greater for girders with rectangular holes than for girders with circular holes for the same size of the holes. The size of the hole must therefore be restricted, see [3].

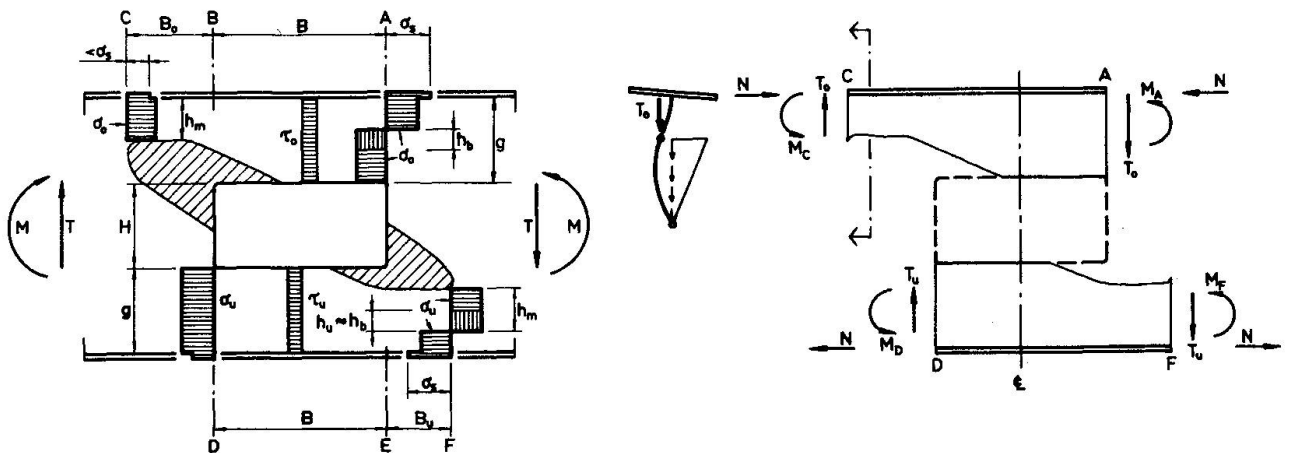


Fig. 15 Model for a girder with a rectangular web hole. Combined bending and shear.

4. ACKNOWLEDGEMENT

This report is based on research work at the Department of Building Statics and Structural Engineering of the Royal Institute of Technology, Stockholm, Sweden. Head of the department is Professor Henrik Nylander whom the author wishes to thank for valuable support. The author also wishes to thank the Swedish Council for Building Research and Gränges Hedlund AB, Stockholm for sponsoring the investigation.

5. REFERENCES

- [1] Rockey, K.C., Andersson, R.G. & Cheung, Y.K. The behaviour of square shear webs having a circular hole. P. 148-172 in Thin walled steel structures, ed. by Rockey and Hill, Crosby Lookwood, 1969.
- [2] Basler, K & Thürlimann, B. Strength of plate girders in bending. Journal Structural Division, ASCE, Aug. 1961.
- [3] Höglund, T. Bärförmåga hos tunnväggig I-balk med cirkulärt eller rektangulärt hål i livet (Strength of thin plate I-girders with circular or rectangular web holes). Bulletin nr 87 of the Division of Building Statics and Structural Engineering, The Royal Institute of Technology, Stockholm 1970. (In Swedish)
- [4] Provisoriska normer för svetsade stålbalkar, Typ HSI (Specifications for the design of welded steel girders, type HSI) Gränges Hedlund AB, Stockholm 1966. (In Swedish)

SUMMARY

This paper deals with an experimental and theoretical study of the strength of statically loaded plate I-girders with circular or rectangular web holes without web stiffeners. Girders with very thin web are treated. The web depth to thickness ratio ranges from 200 to 300. The load-carrying capacity is then delimited by web failure in the postbuckling range.

RESUME

L'auteur présente une étude expérimentale et théorique de la résistance statique des poutres en I non raidies, comportant des ouvertures rondes ou rectangulaires dans les âmes. Il s'agit de poutres à âme très mince, le rapport de la hauteur à l'épaisseur variant entre 200 et 300. La résistance ultime est ainsi limitée par la ruine de l'âme dans le domaine de voilement post-critique.

ZUSAMMENFASSUNG

Dieser Bericht behandelt eine experimentelle und theoretische Untersuchung über die Beanspruchung statisch belasteter Vollwandträger mit runden oder rechteckigen Stegaussparungen, aber ohne Stegaussteifungen. Es werden Träger mit sehr dünnen Stegen untersucht. Das Verhältnis der Stegdicke zur Höhe variiert zwischen 200 und 300. Damit ist die Traglast durch das Versagen des Steges im überkritischen Beulbereich beschränkt.

Leere Seite
Blank page
Page vide